Reports

Dislocations in Ice

Abstract. *The dislocation structures of dendritic ice crystals have been directly observed by x-ray diffraction topography. Growth occurs without the intervention of dislocations and very low dislocation dencities may initially prevail. Straining expands dislocations having* $\langle 11\bar{2}0 \rangle$ *direction Burgers vectors from sources at grown-in inclusions. Slip of these dislocations in the basal plane (0001) and on pyramidal planes, probably* $(1\bar{1}01)$*, with frequent occurrence of primatic punching, is observed. Dislocation reactions of the type* $(a_0/3)\,[11\bar{2}0] + (a_0/3)\,[1\bar{2}10] = (a_0/3)\,[2\bar{1}\bar{1}0]$ *and a strong preference for pure screw orientation are characteristic. These dislocations generally account for the known anisotropy of plastic flow in ice.*

Ice provides an especially interesting set of problems in its plastic deformation which usually occurs very near its melting point, and in its crystal growth which provides an immense variety of phenomena to understand (*1*). Plastic deformation of ice is a current problem of glaciology and the engineering of ice and snow structures. From studies of mechanical properties, crystal growth, and etching, some characteristics of crystalline dislocations in ice have been deduced inasmuch as dislocations provide the principal mechanism for plastic deformation of crystals and often participate in growth processes (*2*).

We have applied x-ray diffraction topography for direct observation of the distribution of dislocations in some ice crystals (*3*). These techniques take advantage of the differences of the x-ray intensities diffracted by perfect crystal lattices and by the imperfect neighborhoods of dislocations. We used a transmission arrangement, devised by Lang (*3*), in which incident x-rays enter one side of a crystal, are diffracted at a small angle from lattice planes crossing the crystal, and leave the crystal through the opposite face. A map of diffracted intensities is recorded on a nuclear emulsion at original size, and the record is subsequently enlarged for inspection. In the photographs presented, higher diffracted intensities, that is, dark lines originally about 5 μ wide, delineate dislocation positions. Since the method senses distortions of the spacing and orientation of the diffracting planes only, the anisotropy of the strain field of dislocations is detected and the orientation of the Burgers vectors of dislocations can be determined. Most of our topographs utilized $\{1\bar{1}00\}$ type diffracting planes. Thus, in any one picture, two of the three possible permutations of the expected $\langle 11\bar{2}0 \rangle$ type Burgers vectors were visible.

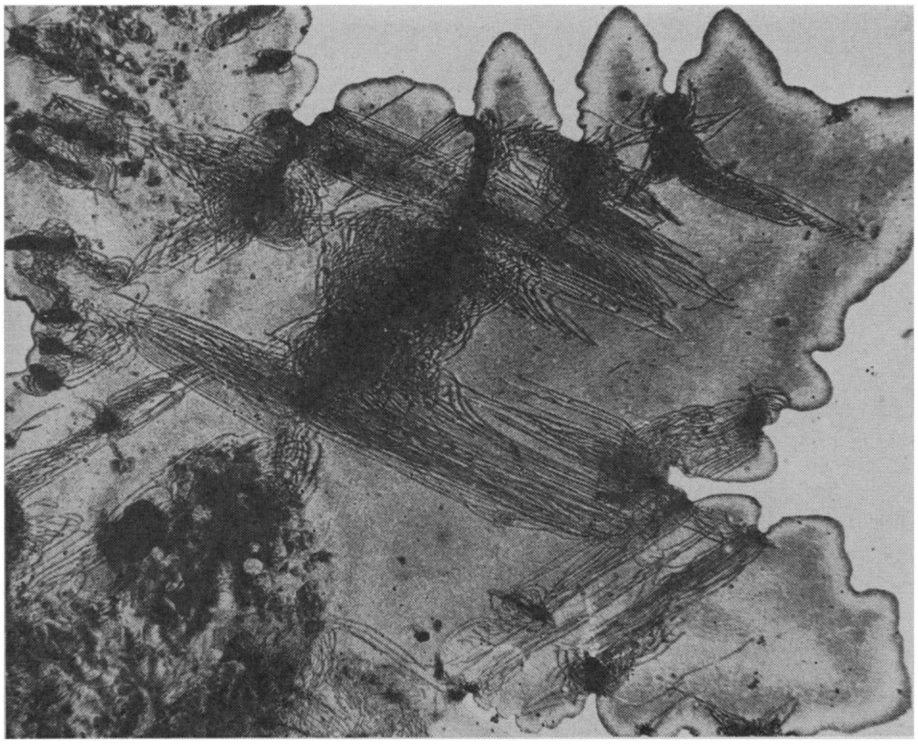

Fig. 1. X-ray diffraction topograph of tabular ice dendrite after gentle straining. Dislocations with Burgers vectors in $[11\bar{2}0]$ and $[1\bar{2}10]$ directions are visible as thin dark lines extending from sources at interdendritic inclusions. Those with $[\bar{2}110]$ Burgers vectors are invisible in this photograph. Regions of the crystal that are smoothly shaded are otherwise virtually perfect. The rounded contours of the crystal edges are due to slight sublimation after crystal growth. About × 15.

The crystals we studied were tabular dendrites about 0.1 to 0.3 mm thick and up to 2 cm in major dimension. The largest surfaces of these crystals were nearly parallel to the basal plane of the hexagonal crystal lattice, and the dendrite growth axes were nominally $\langle 11\bar{2}0 \rangle$ directions. We grew these crystals by supercooling distilled water to between $-0.5°$ and $-1.5°$C and seeding it with a cold metal rod or a massive ice crystal. From the mass of dendrites that formed, one was extracted by breaking away its neighbors and mounted in a cryostatic camera for x-ray topography.

Figure 1 shows part of a diffraction topograph of a branched dendrite with dislocations (thin black lines) extending from sources at interdendritic inclusions. Other results show that these crystals were nearly free of dislocations as grown. The type of dislocation structure shown is developed by gentle straining subsequent to growth. That the regions between dislocations are nearly perfect is demonstrated by the diffuse contrast bands parallel with the crystal edges. These are "pendellosung" fringes, a contrast effect that occurs as a consequence of x-ray interference in perfect crystals (*4*).

Most of the dislocations lie in or nearly parallel with the (0001) planes since they extend for distances many times the crystal thickness. The appearance and vanishing of contrast as diffracting planes are permuted identifies the Burgers vectors of these dislocations as $(a_0/3)\ \langle 11\bar{2}0\rangle$ type. In Fig. 1 only two-thirds of all the dislocations appear since the $\pm\ [\bar{2}110]$ directions vanish with $(01\bar{1}0)$ diffracting planes. The screw orientation is most common, and many dislocations are very nearly straight in the screw orientation. This suggests either a much higher mobility for edge and mixed orientations or a very low energy (Peierls valley) for the screw orientation.

Some cross slip of $<11\bar{2}0>$type dislocations on pyramidal planes of $\{hh01\}$ type, probably, but not necessarily exclusively, $[1\bar{1}01]$ type, is evident at the right hand side of Fig. 1 where some short parallel segments remain of a configuration that has expanded from a source. Some of these dislocations are still attached to screw segments extending out from the source. Others have lost their screw segments by gliding out through the crystal surfaces and remain as short segments threading through the crystal.

Some conclusions that can be drawn from our preliminary observations such as the example described above are:

1) Growth of ice dendrites does not require a dislocation mechanism and nearly dislocation-free crystals can be formed. In some cases dendrite branches have grown together without dislocation formation.

2) The Burgers vectors of dislocations formed by light strain lie in $\langle 11\bar{2}0\rangle$ directions.

3) The basal plane (0001) is the principal slip plane although $\langle 11\bar{2}0\rangle$ type dislocations also cross slip on pyramidal planes, probably $\{1\bar{1}01\}$.

4) The screw orientation is strongly preferred in the basal plane.

5) Dislocation reactions of the type $(a_0/3)\ [11\bar{2}0] + (a_0/3)\ [1\bar{2}10] = (a_0/3)\ [2\bar{1}\bar{1}0]$ are observed.

6) Prismatic punching occasionally originates at the same growth defects from which basal glide dislocations multiply. The presence alone of $\langle 11\bar{2}0\rangle$ type dislocations indicates that basal glide would predominate in macroscopic plastic flow and that dislocation pile-ups would readily nucleate cracks.

These dislocation properties appear to account for the observed plastic anisotropy and brittleness of ice. However, slip by other dislocations with nonbasal Burgers vectors has not been excluded although not observed in these experiments. Etch pit patterns on (0001) surfaces (*5*) show only a small fraction of the dislocations structure visible in diffraction topographs since dislocations tend to lie parallel with (0001) planes.

Dislocation configurations in hexagonal substances with such diverse properties as zinc (*6*) and silicon carbide (*7*) are observed to be remarkably similar to those in ice. Although the temperatures at which the structures form are radically different, they are, in each case, close to the respective melting temperature.

C. E. Hayes*
W. W. Webb
Department of Engineering Physics and Materials Science, and *Laboratory of Atomic and Solid State Physics, Cornell University, Ithaca, New York*

References and Notes

1. W. D. Kingery, Ed., *Ice and Snow* (M.I.T. Press, Cambridge, Mass., 1963), a summary of recent work on ice.
2. For an account of dislocations in crystals, see W. T. Read, *Dislocations in Crystals* (McGraw-Hill, New York, 1953); J. Friedel, *Les Dislocations* (Gauthier-Villars, Paris, 1956); or A. H. Cottrell, *Dislocations and Plastic Flow in Crystals* (Oxford Univ. Press, London, 1953).
3. A. R. Lang, *J. Appl. Phys.* **29**, 597 (1958); *Acta Cryst.* **12**, 249 (1959); for a review, W. W. Webb, in *X-ray Diffraction Topography, Direct Observation of Dislocations,* J. H. Wernick and J. B. Newkirk, Eds. (Wiley, New York, 1961), p. 29.
4. N. Kato, *Acta Cryst.* **14**, 526, 627 (1961); for a review of the appropriate diffraction theory, see R. W. James, *Solid State Phys.* **15, 55** (1963).
5. D. Kuroiwa and W. L. Hamilton, in *Ice and Snow,* W. D. Kingery, Ed. (M.I.T. Press, Cambridge, Mass., 1963), p. 34.
6. A. Fourdeaux, A. Berghezan, W. W. Webb, *J. Appl. Phys.* **31**, 918 (1960).
7. S. Amelinckx, G. Strumane, W. W. Webb, *ibid.,* p. 1359.
8. Based on a project submitted by C.E.H. in partial fulfillment of requirements for the degree of Bachelor of Engineering Physics at Cornell University. We thank J. B. Sayah who set up the diffraction topography apparatus and helped with photography. Supported by the National Science Foundation; some facilities were provided by the Advanced Research Projects Agency.

* Present address: Department of Physics, Harvard University, Cambridge, Mass.

31 August 1964

■

Reversibility of Reaction of Potassium with Liquid Ammonia

Abstract. *Ammoniated electrons exist in solutions of potassium amide in liquid ammonia which have reached thermodynamic equilibrium with hydrogen gas. By determining electron concentrations by electron spin resonance, an equilibrium constant of 10^5 at room temperature has been obtained.*

The correlation of thermodynamic data for electrolytes in liquid ammonia (*1*) made it possible to estimate an equilibrium constant of approximately 10^6 at 25°C for the reaction of the ammoniacal electron (e^-_{am}) with ammonia to form amide and hydrogen:

$$e^-_{am} + NH_3 = NH_2^- + \tfrac{1}{2}\ H_2$$

It was recognized that this equilibrium constant is probably small enough to permit direct measurement of the equilibrium; by using electron spin resonance (ESR), we have recently detected unpaired electrons in potassium amide solutions which were equilibrated with hydrogen partial pressures as low as 0.1 atm.

Measured amounts of potassium metal and ammonia were sealed in Pyrex glass tubes (4 mm × 20 cm), and the tubes were allowed to stand at room temperature. Several days after the deep blue color of the potassium solutions had been replaced by the yellow color of the potassium amide solutions, distinct ESR spectra were observed with a Varian V-4502 EPR spectrometer. The spectra were single resonances of very narrow half-width (~0.06 gauss) with a Landé *g*-value of 2.0010; the close agreement of these parameters with those observed by Hutchison and Pastor (*2*) for potassium solutions makes it certain that the spectra correspond to the ammoniacal electron. Several data indicate that true equilibrium was achieved. (i) The intensities of the spectra of solutions kept at room temperature did not change during periods as long as 3 months. (ii) Raising the temperature of a solution caused the electron concentration to increase, and cooling caused the electron concentration to decrease (*3*). After returning a solution to room temperature, the electron concentration returned to its original value in a period of about 1 day. (iii) A tube fitted with break-seals containing an equilibrated solution was opened, and most of the hydrogen was removed. After re-equilibration, a markedly weaker ESR signal

Table 1. Equilibrium data for ammonia solutions at room temperature.

Concn. of amide ion (M)	P_{H_2} (atm)	Concn. of electron ($10^{-5}\ M$)	$\dfrac{P_{H_2}{}^{1/2}(NH_2^-)}{(e^-)} \times 10^{-5}$
0.50	23.2	0.54	4.5
.57	11.9	.42	4.7
.81	28.5	.52	8.3
.99	19.6	.52	8.4
1.26	27.1	.56	12
1.56	23.2	.46	16